doi: 10.3969/j.issn.0490-6756.2019.01.018

由 Rashba 效应和横向自旋轨道耦合诱发的量子点接触中的 0.7 反常结构研究

王紫江, 寇清臣, 高瑞彦, 何建红, 郭华忠, 于白茹
(四川大学物理科学与技术学院, 成都 610064)

摘 要: 本文研究了在非对称限制势下由 Rashba 效应和横向自旋-轨道耦合诱发的量子点接触系统中的反常量子输运行为. 研究发现,在一定范围的 Rashba 相互作用强度下,电导在 $0.8\times 2e^2/h$ 附近有一个较弱的坪台. 该坪台电导的值与非对称限制势的偏压有关. 在某个范围的偏压下,它会随着偏压的增大而减小. 另外,由于 Rashba 自旋-轨道耦合效应,在非对称限制势作用下电子将会自旋极化. 因此, 在没有任何外加磁场的情况下, 采用纯电学手段即可做成量子点接触自旋偏振器.

关键词: 量子点接触; 0.7 反常结构; Rashba 相互作用
中图分类号: O471 **文献标识码**: A **文章编号**: 0490-6756(2019)01-0095-09

Investigations of 0.7 anomaly due to Rashba effect and lateral spin-orbit coupling in the quantum point contacts

WANG Zi-Jiang, KOU Qing-Chen, GAO Rui-Yan, HE Jian-Hong, GUO Hua-Zhong, YU Bai-Ru
(College of Physical Science and Technology, Sichuan University, Chengdu 610064, China)

Abstract: We study the abnormal quantum transport through quantum point contact systems with Rashba effect and lateral spin-orbit coupling under asymmetric confinement geometries. We find that for a certain range of Rashba interaction strength, the conductance has a weak plateau around $0.8\times 2e^2/h$. The value of this anomalous plateau is dependent on the voltage bias of the asymmetric confinement. We find that for a certain range of voltage bias, this weak plateau is lowered slightly with increasing the voltage bias. Furthermore, we find that the asymmetric confinement gives rises to a nonzero spin polarization due to the Rashba spin-orbit coupling. Therefore, we can make such quantum point contact spin-polarizer by purely electrical means in the absence of any applied external magnetic field.

Keywords: Quantum point contacts; 0.7 anomaly; Rashba interaction

1 Introduction

The study of electronic transport in split-gates quantum point contacts (QPC) is an active field of research. The theoretical approach of conductance from transmission in a ballistic conductor was firstly investigated by Landauer[1,2]. Then Büttiker extended the theory to multi-lead system[3], resulting in the Landauer-Büttiker formalism. The quantized conductance of QPC was

收稿日期: 2018-01-26
基金项目: 国家重点研发项目(2016YFF0200403); 国家自然科学基金重点项目(11234009)
作者简介: 王紫江(1993-), 男, 北京市人, 硕士生, 研究方向为介观与低维物理.
通讯作者: 郭华忠. E-mail: guohuazhong@scu.edu.cn; 于白茹. E-mail: yubrscu@126.com

first experimentally confirmed in 1988[4,5]. When a negative voltage is applied on the metal split gates, the two-dimensional electron gas (2DEG) is depleted underneath the gates and forms one-dimensional channel. If the length of the channel is short enough compared to the mean free length, the transport of electrons is ballistic. By controlling the applied gate voltage, we can control the width of the one-dimensional channel in the QPC, while the QPC's conductance is a function of the width of the channel, and the conductance is quantized in units of $G_0 = 2e^2/h$.

There are many theoretical models for the quantized conductance in QPC in the linear-response regime. Assuming an adiabatic change in the geometry will theoretically predict plateaus in conductance without resonant structure[6].

Besides integer plateaus of conductance in units of G_0, there are some other features in the conductance of QPCs. Thomas *et al*. firstly addressed specifically an anomalous plateau typically observed at 0.7 G_0[7], which is usually called 0.7 anomaly. 0.7 anomaly appears in the conductance of QPCs universally, and it can't be explained by single-particle transport theory. There are many theoretical explanations for 0.7 anomaly, including spontaneous spin polarization[7], Kondo physics[8-10], Wigner crystallization[11,12], phenomenological spin-gap models[13] *etc*. Although the physical mechanism for 0.7 anomaly is the subject of extensive debate, we can determine that it is a many-body effect.

When considering the transport in 2DEG, the spin-orbit (SO) coupling could have a great impact on the dynamics of carriers and their spins. Hsiao *et al*. consistently explained 0.7 G_0 plateaus by the Rashba interaction[14]. They explained that the Rashba interaction strength is proportional to the nonuniform electric field E in the z direction perpendicular to the 2DEG plane in the GaAs/AlGaAs heterostructure. An effective potential well will be formed due to the Rashba interaction term, and when the well is sufficiently deep it is able to trap electrons so as to provide the local magnetic moment for the Kondo effect.

Transport properties of 2DEG in the presence of SO coupling have been reported in literature[15], including QPC structures[16, 17]. Hsiao *et al*. established the relationship between 0.7 anomaly and the Rashba interaction, but the resulted conductance as function of the gate voltage was not provided[14]. Among the countless investigations on 0.7 anomaly, it is hard to find one that confirmed the correlation between 0.7 anomaly and the Rashba interaction by offering numerical results of the conductance with a 0.7-anomaly-like structure.

We here provide a method to numerically calculate the conductance of ballistic system with Rashba interaction and lateral spin-orbit coupling induced by a lateral confinement potential. Especially, by adjusting the Rashba interaction strength, we obtain a 0.8 G_0 plateau. This plateau is dependent significantly on the voltage bias between the split gates. We find that for a certain range of voltage bias, with increasing the bias, this weak plateau is lowered slightly. The asymmetric confinement gives rise to a nonzero spin polarization due to the Rashba interaction. Calculations show that we can make such quantum point contact spin-polarizer by purely electrical means in the absence of any applied external magnetic field.

2 Theoretical model

We consider a two-dimensional system in which a 2DEG is confined in a plane perpendicular to the z axis. The longitudinal direction is defined as the x direction, and the transverse direction is defined as the y direction. The split gates of QPC is on the surface of the device and the distance from the 2DEG to the QPC's surface gate is d.

We model the electrostatics around the channel region with Davis' method[19]. In our calculations, we use this model to calculate the potential applied on the 2DEG, and put it into the Hamiltonian to calculate the scattering matrix. The electrostatic potential of an infinite triangle gate

with one edge along the x axis whose vertex at the origin includes an angle $2A$ is given by:

$$V(x,y,d,A,Vg)=\frac{V_g}{\pi}\arctan\frac{d\sin A}{(R-x)\cos A-y\sin A} \tag{1}$$

where x and y are the two-dimensional coordinates, d is the distance from the 2DEG to the QPC's surface gate, V_g is the voltage applied on the gates, and $R=\sqrt{r^2+d^2}$.

In our model, to describe QPCs we adopt a pair of triangular split gates which include a top gate and a bottom gate on the surface of the AlGaAs/GaAs heterostructure. The 2DEG is assumed to be an ideal plane under the surface of the QPC. The distance from the 2DEG to the QPC's surface is d. The scattering region is in a shape of rectangle with a width of 1500 nm and a length of 2000 nm. The channel for conducting electrons is parallel to x axis. Each gate is in the shape of an equilateral triangle, and their shapes are symmetrical about the x axis. The shortest distance between vertexes of the two gates is 300 nm, and the height of each equilateral triangle is 2000 nm. Fig. 1(a) shows the sketch of the scattering region. The two red triangles represent the surface split gates. The channel for conducting electrons is formed when the 2DEG underneath the surface gates was depleted, and P denotes the momentum of conducting electrons. We introduce a '*deltaV*' term as the bias shift between the top and bottom gates. In this case, the potential on the top gate is V_g whereas the potential on the bottom gate is $V_g+deltaV$. The potential generated by the split gates can be written as:

$$V''(x,y,d)=V'(x,y-\frac{gap}{2},d,V_g)+V'(x,-y+\frac{gap}{2},d,V_g+deltaV) \tag{2}$$

where gap is the shortest distance between vertexes of the two gates that is 300 nm, and function $V'(x,y,d,V_g)$ is the potential generated by one upside-down equilateral triangle gate which is shown as triangle BCO in Fig. 1(b). The triangle gate BCO in Fig. 1(b) can be obtained by subtracting infinite triangle gate EOD and ABF from AOD and then adding another infinite triangle gate ECF. Since the potential can be added or subtracted linearly as gates[19], we can do the same thing as above to get the potential generated by triangle BCO. Therefore $V'(x,y,d,V_g)$ can be derived and written as:

$$V'(x,y,d,V_g)=V(x,y,d,\frac{\pi}{3},V_g)-V(x,y,d,\frac{\pi}{6},V_g)-V(x+\frac{h}{\sqrt{3}},y-h,d,\frac{\pi}{3},V_g)+V(x-\frac{h}{\sqrt{3}},y-h,d,\frac{\pi}{6},V_g) \tag{3}$$

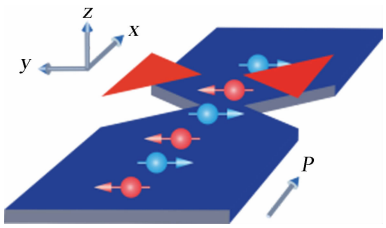

(a)

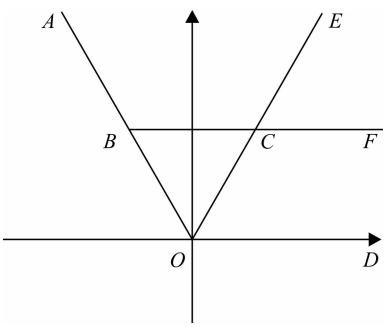

(b)

Fig. 1 (a) Sketch of the scattering region, the channel for conducting electrons is formed when the 2DEG underneath the surface gates was depleted; (b) sketch of an upside-down equilateral triangle gate BCO

where h is the height of the equilateral triangle and V is the function in Eq. (1). With these parameters we can calculate the potential $V(x,y,d)$. Fig. 2(a) is the potential at a depth of 100 nm calculated by Eq. (2) with $V_g=4.2$ V and a zero bias and Fig. 2(b) is the potential with $V_g=4.2$ V and $deltaV=-1.5$ V.

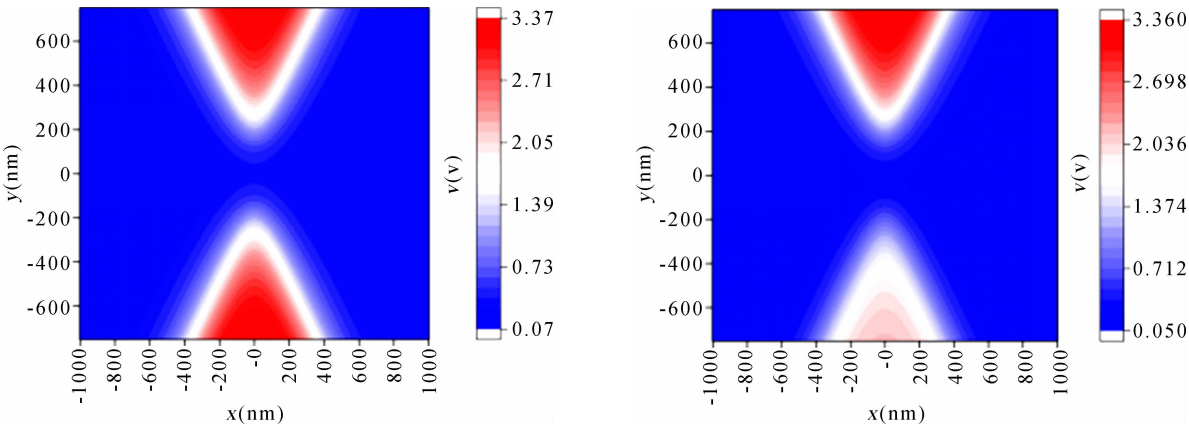

Fig. 2 Color map of potential calculated by Eq. (3) with V_g=4.2 V and (a) a zero bias; (b) the potential with V_g=4.2 V and *deltaV*=−1.5 V

The usual Rashba interaction associated with the interfacial electric field is given by[18]:

$$H_{SO}^{R}=\frac{\alpha}{\hbar}(\sigma_x P_y-\sigma_y P_x) \tag{4}$$

where σ_x and σ_y are Pauli matrices, P_x and P_y denote the kinetic momentum, and α denotes the spin-orbit coupling strength. It is a spin-orbit coupling term induced by the electric field in the z direction due to the heterostructure band alignments and surface gates.

When the '*deltaV*' term is nonzero, the resulted confinement potential is asymmetric. The asymmetric field gives rise to a lateral spin-orbit interaction (LSOC) which further couples the spin and orbital degrees of freedom[20,21]. This lateral SO potential takes the form[22]:

$$V_{SO}^{\beta}=-\frac{\beta}{\hbar}\vec{\nabla}U(x,y,z)\cdot(\vec{\sigma}\times\vec{P}) \tag{5}$$

where $\beta=\hbar^2/4m^{*2}c^2$ and $\vec{\sigma}=(\sigma_x,\sigma_y,\sigma_z)$. m^* is the effective mass of conducting electrons. $U(x,y,z)$ is the potential energy of electrons and can be derived from V'' in Eq. (2) (z=0 corresponds to the surface of QPC, so $d=-z$):

$$U(x,y,z)=-eV''(x,y,-z) \tag{6}$$

The total Hamiltonian is then given by:

$$H=\frac{(P_x^2+P_y^2)}{2m^*}+H_{SO}^{R}+U(x,y,z)+V_{SO}^{\beta} \tag{7}$$

In our model, the leads' directions are parallel to the x axis and they are semi-infinite, while in the y direction there is a hard-wall boundary condition. For simplicity of calculation, the SO coupling α is set to zero at the infinite leads but is turned on at the scattering region. We use a python package-Kwant-to calculate the wave functions and conductance[23] within the frame of tight-binding approximation. The distance between nearest lattice points is set as a. The coordinates of every lattice point (μ, ν) correspond to real-space coordinates ($a\mu$, $a\nu$).

In order to calculate the transmission, we have to obtain the discretized Hamiltonian. The system is described by the two-dimensional Schrödinger equation

$$H=H_0+H_{SO}^{R}+V_{SO}^{\beta}=-\frac{\hbar^2}{2m^*}(\partial_x^2+\partial_y^2)+U(x,y,d)+H_{SO}^{R}+V_{SO}^{\beta} \tag{8}$$

Introducing the discretized positional states

$$|\mu,\nu\rangle=|a\mu,a\nu\rangle=|x,y\rangle \tag{9}$$

in the limit $a\to 0$, the partial derivative operators can be expressed as

$$\partial_x=\frac{1}{2a}\sum_{\mu,\nu}(|\mu+1,\nu\rangle\langle\mu,\nu|-|\mu,\nu\rangle\langle\mu+1,\nu|) \tag{10}$$

and an equivalent expression for ∂_y. Substituting it in the discretized Hamiltonian gives

$$H=\sum_{\mu,\nu}[(U(a\mu,a\nu,z)+4t)|\mu,\nu\rangle\langle\mu,\nu|-t(|\mu+1,\nu\rangle\langle\mu,\nu|+|\mu,\nu\rangle\langle\mu+1,\nu|+|\mu,\nu+1\rangle\langle\mu,\nu|+|\mu,\nu\rangle\langle\mu,\nu+1|)]+\sum_{\mu,\nu}\left[\left(i\beta\frac{\partial U(a\mu,a\nu,z)}{\partial z}-\frac{i\alpha}{2a}\right)\sigma_x-i\beta\frac{\partial U(a\mu,a\nu,z)}{\partial x}\sigma_z\right](|\mu,\nu+1\rangle\langle\mu,\nu|-$$

$$|\mu,\nu\rangle\langle\mu,\nu+1|)+\sum_{\mu,\nu}\left[\left(-i\beta\frac{\partial U(a\mu,a\nu,z)}{\partial z}+\frac{i\alpha}{2a}\right)\sigma_y+i\beta\frac{\partial U(a\mu,a\nu,z)}{\partial y}\sigma_z\right](|\mu+1,\nu\rangle\langle\mu,\nu|-|\mu,\nu\rangle\langle\mu+1,\nu|) \tag{11}$$

where $t=\hbar^2/2m^*a^2$. For a smaller a, the discretized Hamiltonian approximates the continuous Hamiltonian to a higher accuracy. The approximation is good enough for quantum states of Fermi wave length much larger than a. Hence $a\ll\lambda_f$, and we get $t=\hbar^2/2m^*a^2\gg\hbar^2/2m^*\lambda_f^2$. According to De Broglie formula $\lambda=h/p$, we get $t\gg p^2/8\pi^2m^*=E_f/4\pi^2$, which leads to $E_f\ll 4\pi^2t$.

In our simulation the Fermi energy is set to be lower than t. For simplicity, in our model we set $t=1$. Thus the unit of energy is $t=\hbar^2/2m^*a^2$.

Kwant uses Python codes to define the tight-binding discretized Hamiltonian. First we define the type of the system's lattice and the shape of scattering region, and then define the onsite and hopping in the Hamiltonian. We use non-atomistic model in our calculation. For the simulation of 2DEG system we use a two-dimensional mesh with spacing $a=5$ nm. Considering spin-dependent conductances, we calculate the spin polarization by the current polarization

$$P=\frac{G^{\uparrow\uparrow}+G^{\uparrow\downarrow}-(G^{\downarrow\uparrow}+G^{\downarrow\downarrow})}{G^{\uparrow\uparrow}+G^{\uparrow\downarrow}+G^{\downarrow\uparrow}+G^{\downarrow\downarrow}}=\frac{G^{\uparrow}-G^{\downarrow}}{G^{\uparrow}+G^{\downarrow}} \tag{12}$$

3 Results and discussion

We present results for a QPC, using the parameters stated below. The distance from the surface gate to 2DEG is $d=100$ nm. To calculate transmission function we need the Fermi energy of electron E_f. In all our calculations the energy unit is t, $t=\hbar^2/2m^*a^2$. We consider 2DEG made out of GaAs/AlGaAs heterostructure, thus $m^*=0.067m_e$. We set $E_f=0.24t\approx 0.0054$ eV, which corresponds to an electron density n_S about $4.8\times10^{10}\ e^-/\mathrm{cm}^2$. According to Ref. [24], the value for α in Ⅲ-Ⅴ semiconductors is no more than a few 10^{-11} eV·m. In our calculation the spin-orbit coupling strength α is around 9.67×10^{-11} eV·m and β is around 5×10^{-17} m^2.

In our results, the unit of voltage will be the energy unit t. Fig. 3 shows curves of conductance G as function of the top gate voltage V_g under the last second integer plateau. Each curve corresponds to a different *deltaV* of the Davies's potential. The rightmost curve on the left of the break point corresponds to $deltaV=2.2t$ whilst the leftmost curve corresponds to $deltaV=2.6t$. Fig. 3 also shows the curve with $deltaV=0$ as a reference. For the left five curves, the difference of *deltaV* between two adjacent curves is $0.1t$. The left five curves are arranged from right to left with an almost constant spacing of V_g, which can be explained by electrostatics. For a same V_g, the bottom gate voltage rises by increasing *deltaV* while the top gate voltage is fixed. As *deltaV* is positive, a larger *deltaV* leads to a more open quasi-1D channel, which in turn results in a larger G. It can be also concluded that the curve with a larger *deltaV* has a more negative pinch-off voltage V_g.

Fig. 3 also shows that each curve has a shoulder-like plateau around $0.8G_0$, which is accounted for the Rashba interaction term H_{SO}^R. This shoulder-like short plateau looks just like the 0.7 anomaly. We also find that the exact conductance value of the 0.7 anomaly is dependent on the spin-orbit coupling strength α, although the results is not presented here. We can find that with increasing the bias between top and bottom gates, the 0.7 anomaly is lowered slightly. For $deltaV=2.2t$, the 0.7 anomaly is a little more than $0.8G_0$, while for $deltaV=2.6t$ it is some value between $0.7G_0$ and $0.8G_0$. For other value of *deltaV*, this conductance changes in a mode that I have not figured out. These results prove that 0.7 anomaly is dependent significantly on the bias between the split gates when introducing the lateral SO potential. The origin of this dependence is obvious, since the lateral SO potential introduces electric field $-\vec{\nabla}V$ in the term V_{SO}^{β} and

$-\vec{\nabla}V$ is related to the bias.

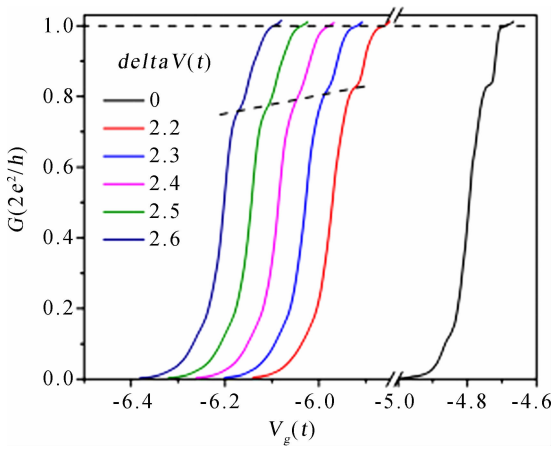

Fig. 3 Conductance as function of the top gate voltage with different *deltaV*s.

We have also studied the relation between the spin polarization and *deltaV* as shown in Fig. 4. In Fig. 4(a), we show conductance curves of spin-up, spin-down and the sum with different *deltaV*s. In the case of symmetric confinement (*deltaV*=0), the spin polarization is zero, whereas the asymmetric confinement obtained a nonzero spin polarization as shown in Fig. 4(b). When G is below G_0, the maximum current polarization P is around 0.08. The contrast between the results of symmetric and asymmetric potential landscapes shows that the lateral spin-orbit coupling or the Rashba interaction is responsible for the appearance of polarization.

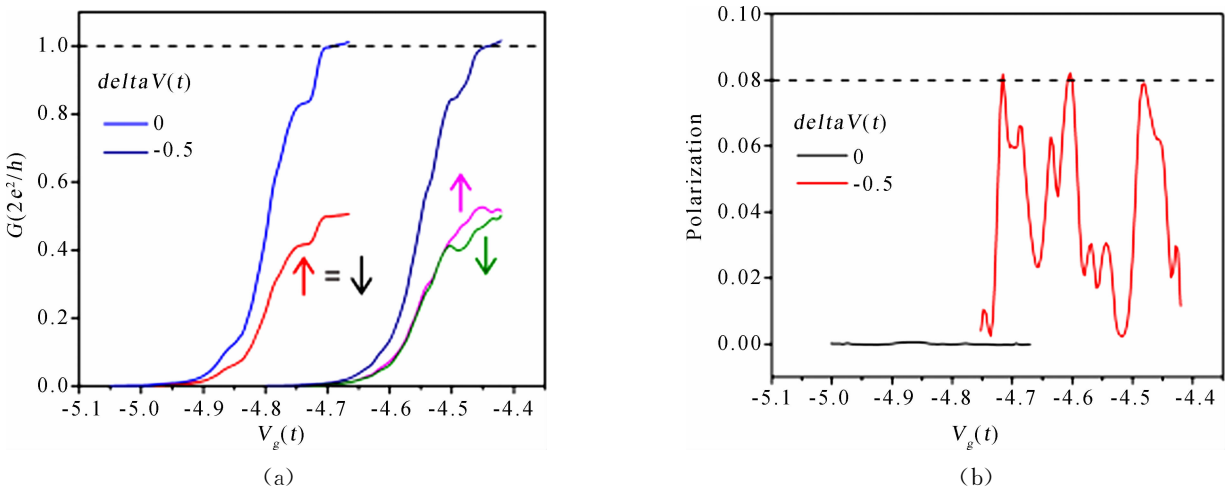

Fig. 4 (a) Spin-dependent conductance curves with different *deltaV*s; (b) the current polarization P with different *deltaV*s

One possible origin for the polarization under asymmetric potential landscape can be attributed to the effective magnetic field $\vec{B}_{SO}$ induced by the LSOC[25]. $\vec{B}_{SO}$ can be deduced by

$$V_{SO}^{\beta}=-\beta\vec{\sigma}\cdot(\vec{k}\times\vec{\nabla}U)=-\beta\vec{\sigma}\cdot(\vec{k}\times\vec{E})=\vec{\sigma}\cdot\vec{B}_{SO}$$

where U is the confinement potential energy, $\beta=\hbar^2/4m^{*2}c^2$, $\vec{B}_{SO}$ is proportional to $\vec{k}\times\vec{E}$.

As shown in Fig. 5, $\vec{B}_{SO}$ has opposite directions at the opposite transverse edges of QPC due to the opposite directions of the electric field $\vec{E}$ in the transverse direction. This will result in an accumulation of electrons with opposite spin directions at opposite transverse edges as shown in Fig. 5(a). This is the signature of the spin Hall effect. When the potential energy of one edge, for example the right edge as shown in Fig. 5(b), is lowered, the potential becomes the asymmetric full line from the dashed line. Major spin-up electrons on the right edge experience less scattering. Thus the spin-up current exceeds the spin-down current.

On the other hand, studies have shown that the Rashba interaction has a similar spin Hall accumulation effect[26,27]. The authors of Ref. [27] calculated nonequilibrium spin density in the 2DEG strap based on the Rashba SO coupling model and found that the spin density is polarized along the opposite directions at both edges of the strap. In our model, we need to differentiate either the Rashba SO coupling or the LSOC dominates in the spin polarization effect.

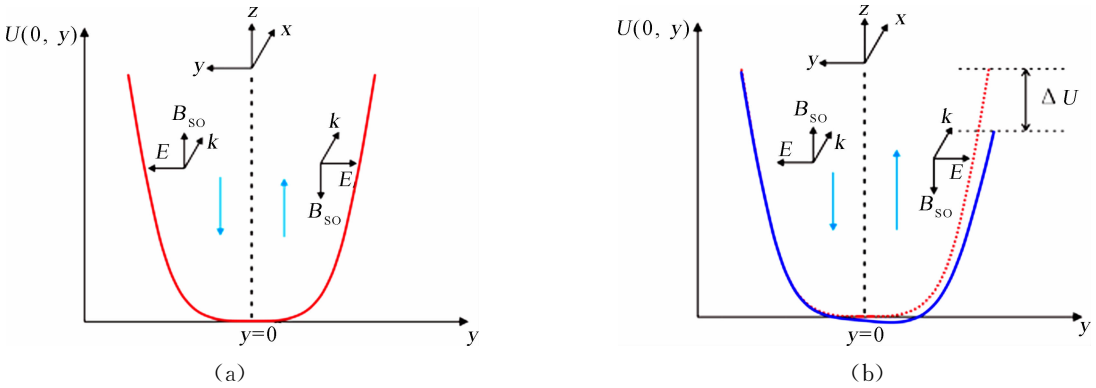

Fig. 5　(a) Schematic representation of the potential energy U in the transverse direction at $x=0$ for a symmetric potential landscape; (b) the potential energy for an asymmetric potential landscape. The dashed line is potential energy for a symmetric potential landscape.

The polarization of spins and the accumulation of electrons in the real space can be investigated from the transmitted wave-function square modulus. Fig. 6(a) shows the calculated normalized spin-up and spin-down transmitted wave-function square modulus when α is around 9.67×10^{-11} eV · m and β is zero and Fig. 6(b) shows the normalized spin-up and spin-down transmitted wave-function square modulus when α is zero and β is around 5×10^{-17} m^2. In both cases V_g is set to be around the $0.7G_0$ region (where the spin polarization is obvious in the conductance curves for a none zero *deltaV* in Fig. 4). In Fig. 6(a) *deltaV* is zero while in Fig. 6(b) *deltaV* is $0.5t$. In Fig. 6(a), we find a clear signature of the accumulation polarization of the opposite spins at the opposite edges of the conducting channel, whereas in Fig. 6(b) there does not exist a similar phenomenon. These calculations prove that the Rashba interaction strength is essential in generating spin-dependent currents polarization when the split gates are biased. From Fig. 6(a) we find that in the QPC channel spin-down density is more concentrated on the up edge while the spin-up density is more concentrated on the down edge. When *deltaV* is zero, the QPC channel locates at $y=0$, and the confining potential has a symmetric effect on the spin-up and spin-down electron waves. Thus the spin-up conductance equals to spin-down conductance. When *deltaV* is not zero, the confining potential has different influence on the wave function of spin-up and spin-down electrons, leading to a spin polarization. On the other hand, the LSOC does not show an effect of polarizing the spin, even with an asymmetric potential, as shown in Fig. 6(b). One possible reason may be that the LSOC is too weak to influence the conducting electrons due to a small absolute value of *deltaV*.

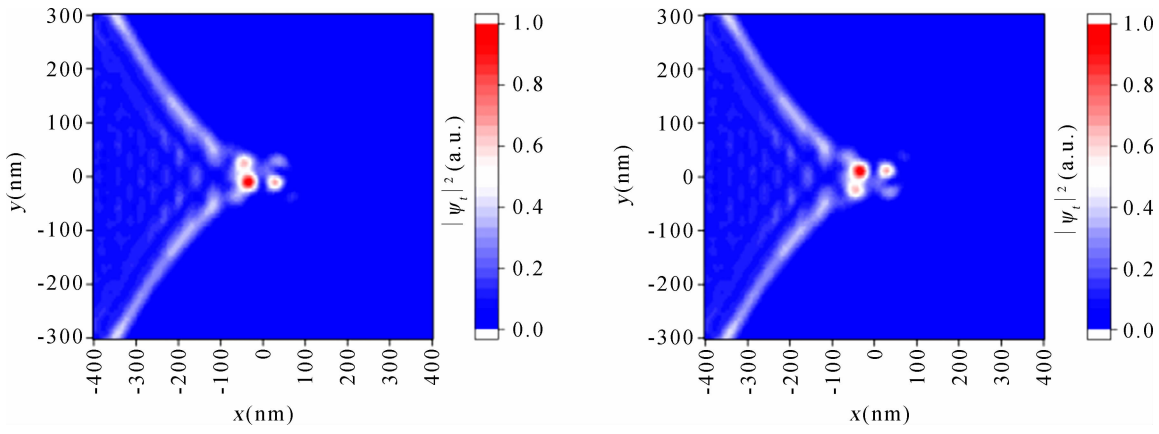

(a)

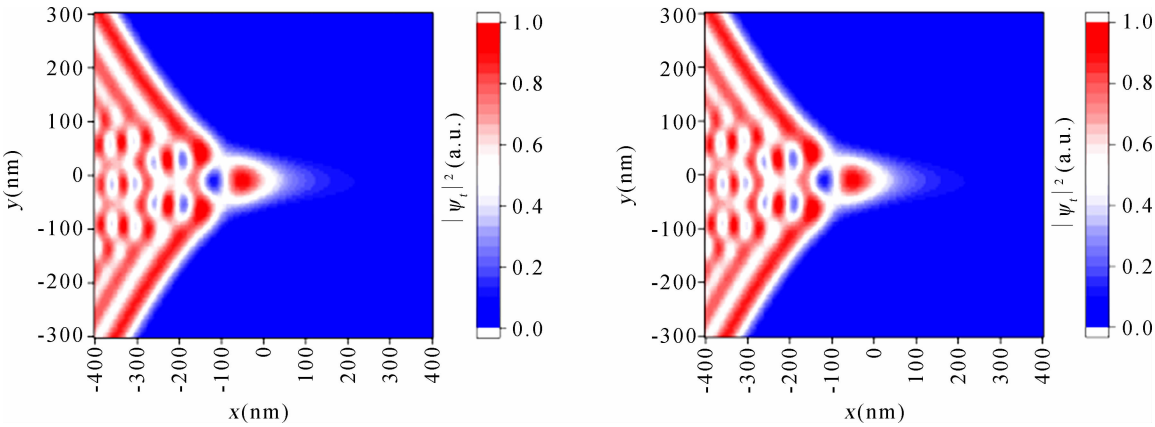

Fig. 6 (a) Normalized transmitted wave-function square modulus (left for the spin-up and right for the spin-down) when V_g is in the region of around $0.7G_0$. The α is around 9.67×10^{-11} eV · m, β and $deltaV$ is zero; (b) The same as (a) while the α is zero, β is around 5×10^{-17} m^2, $deltaV$ is $0.5t$.

It can be deduced that with a reversed asymmetric potential the spin-dependent conductance is reversed too. This effect is shown in Fig. 7. In Fig. 7, we show conductance curves of spin-up, spin-down and the sum with $deltaV=1.5t$, and the equivalent curves with a reversed potential. The spin-orbit coupling strength α is around 9.67×10^{-11} eV · m and β is around 5×10^{-17} m^2. In Fig. 7, each curve is the coincidence of two curves. The spin-up conductance with $deltaV=-1.5t$ is almost equal to spin-down conductance with $deltaV=1.5t$, whereas spin-up conductance with $deltaV=1.5t$ is almost equal to spin-down conductance with $deltaV=-1.5t$. Note that in our numerical results, there is a shift of gate voltage between $deltaV=-1.5t$ and $deltaV=1.5t$ curves, because our bias $deltaV$ is only applied on the bottom gate while the gate voltage is applied on both gates. Considering the voltage shift, we have processed our data so that three pairs of curves coincide.

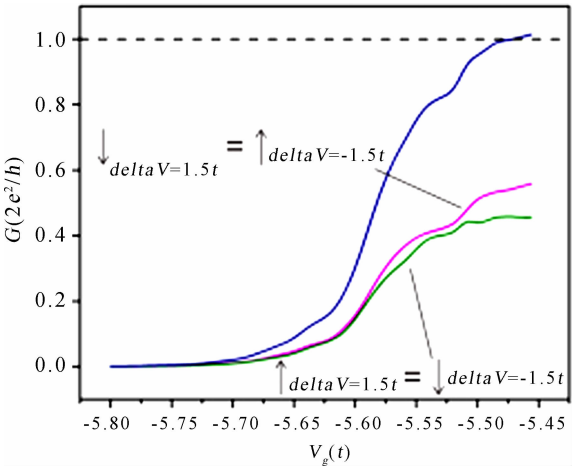

Fig. 7 The spin-dependent conductance curves with $deltaV=1.5t$ and $deltaV=-1.5t$. In this figure we have considered the voltage shift.

4 Conclusions

In summary, our calculation demonstrates that for a reasonable Rashba interaction strength, the Rashba effect can generate a weak plateau around $0.8 \times 2e^2/h$ in the conductance of a QPC system. Furthermore, when introducing a lateral SO potential, this weak plateau is dependent significantly on the bias between the split gates. We find that for a certain range of bias, with increasing the bias, this weak plateau is lowered slightly. The asymmetric confinement gives rise to a nonzero spin polarization due to the Rashba interation. With a reversed asymmetric potential the spin-dependent conductance is reversed too.

References:

[1] Landauer R. Spatial variation of currents and fields due to localized scatterers in metallic conduction [J]. IBM J Res Dev, 1957, 1: 223.

[2] Landauer R. Electrical transport in open and closed systems [J]. Z Phys B: Condens Matter, 1987, 68: 217.

[3] Büttiker M. Four-terminal phase-coherent conductance [J]. Phys Rev Lett, 1986, 57: 1761.
[4] van Wees B J, van Houten H, Beenakker C W J, *et al*. Quantized conductance of point contacts in a two-dimensional electron gas [J]. Phys Rev Lett, 1988, 60: 848.
[5] Wharam D A, Thornton T J, Newbury R, *et al*. One-dimensional transport and the quantization of the ballistic resistance [J]. J Phys C, 1988, 21: L209.
[6] Patel N K, Nicholls J T, Martin-Moreno L, *et al*. Evolution of half plateaus as a function of electric field in a ballistic quasi-one-dimensional constriction [J]. Phys Rev B, 1991, 44: 13549.
[7] Thomas K J, Nicholls J T, Simmons M Y, *et al*. Possible spin polarization in a one-dimensional electron gas [J]. Phys Rev Lett, 1996, 77: 135.
[8] Cronenwett S M, Lynch H J, Goldhaber-Gordon D, *et al*. Low-temperature fate of the 0.7 structure in a point contact: a Kondo-like correlated state in an open system [J]. Phys Rev Lett, 2002, 88: 226805.
[9] Meir Y, Hirose K, Wingreen N S. Kondo model for the "0.7 anomaly" in transport through a quantum point contact [J]. Phys Rev Lett, 2002, 89: 196802.
[10] Rejec T, Meir Y. Magnetic impurity formation in quantum point contacts [J]. Nature, 2006, 442: 900.
[11] Matveev K A. Conductance of a quantum wire at low electron density [J]. Phys Rev B, 2004, 70: 245319.
[12] Brun B, Martins F, Faniel S, *et al*. Wigner and Kondo physics in quantum point contacts revealed by scanning gate microscopy [J]. Nat Commun, 2014, 5: 4290.
[13] Kristensen A, Bruus H, Hansen A E, *et al*. Bias and temperature dependence of the 0.7 conductance anomaly in quantum point contacts [J]. Phys Rev B, 2000, 62: 10950.
[14] Hsiao J H, Liu K M, Hsu S Y, *et al*. 0.7 anomaly due to the Rashba interaction in a nonuniform electric field [J]. Phys Rev B, 2009, 79: 033304.
[15] Ngo A T, Villas-Bôas J M, Ulloa S E. Spin polarization control via magnetic barriers and spin-orbit effects [J]. Phys Rev B, 2008, 78: 245310.
[16] Eto M, Hayashi T, Kurotani Y. Spin polarization at semiconductor point contacts in absence of magnetic field [J]. J Phys Soc Jpn, 2005, 74: 1934.
[17] Reynoso A, Usaj G, Balseiro C A. Detection of spin polarized currents in quantum point contacts via transverse electron focusing [J]. Phys Rev B, 2007, 75: 085321.
[18] Bychov Y A, Rashba E I. Oscillatory effects and the magnetic susceptibility of carriers in inversion layers [J]. J Phys C, 1984, 17: 6039.
[19] Davis J H, Larkin I A, Sukhorukov E V. Modeling the patterned two-dimensional electron gas: Electrostatics [J]. J Appl Phys, 1995, 77: 4504.
[20] Jiang Y, Hu L. Kinetic magnetoelectric effect in a two-dimensional semiconductor strip due to boundary-confinement-induced spin-orbit coupling [J]. Phys Rev B, 2006, 74: 075302.
[21] Xing Y, Sun Q-F, Tang L, *et al*. Accumulation of opposite spins on the transverse edges of a two-dimensional electron gas in a longitudinal electric field [J]. Phys Rev B, 2006, 74: 155313.
[22] Winkler R. Spin-orbit coupling effects in two-dimensional electron and hole systems [M]. Berlin: Springer, 2003.
[23] Groth C W, Wimmer M, Akhmerov A R, *et al*. Kwant: a software package for quantum transport [J]. New J Phys, 2014, 16: 063065.
[24] Schliemann J, Egues J C, Loss D. Nonballistic spin-field-effect transistor [J]. Phys Rev Lett, 2003, 90: 146801.
[25] Wan J, Cahay M, Debray P, *et al*. Possible origin of the 0.5 plateau in the ballistic conductance of quantum point contacts [J]. Phys Rev B, 2009, 80: 155440.
[26] Nikolić B K, Souma S, Zârbo L P, *et al*. Nonequilibrium spin Hall accumulation in ballistic semiconductor nanostructures [J]. Phys Rev Lett, 2005, 95: 046601.
[27] Jiang Y, Hu L. Kinetic magnetoelectric effect in a two-dimensional semiconductor strip due to boundary-confinement-induced spin-orbit coupling [J]. Phys Rev B, 2006, 74: 075302.

引用本文格式：
中　文：王紫江，寇清臣，高瑞彦，等. 由 Rashba 效应和横向自旋轨道耦合诱发的量子点接触中的 0.7 反常结构研究 [J]. 四川大学学报：自然科学版，2019，56：95.
英　文：Wang Z J, Kou Q C, Gao R Y *et al*. The preparation of insoluble humic acid and its adsorption capacity [J]. J Sichuan Univ: Nat Sci Ed, 2019, 56: 95.